

Stanisław DOWNAR\*  
Aleksandr JAKIMOWICZ\*  
Katarzyna MISZCZANKA\*  
Andrzej JAKUBOWSKI\*\*  
Leszek CHYBOWSKI\*\*

## LOAD SIMULATION OF THE PARTHENON FACADE USING FINITE ELEMENT METHOD

*Paper concerns to contact simulation by the finite element method for “freely piled solids” systems. The antique facade of the Parthenon temple is taken for simulation as an example. Marble drums and blocks are held together only by gravity and friction. Multiplicity of contact pressure patterns inside columns are disclosed. Surface compression concentrators between echinus and top drums are revealed. Contact sliding in the column joints is investigated. Sliding localization on the top and bottom of columns is pointed out as a predictor of the uncontrolled movement in the case of the facade inclination.*

### INTRODUCTION

The work concerns the simulation of *load-bearing systems* (LBS) by the finite element method (FEM, FEA) [1]. A special class of LBS is investigated – the *freely piled solids* (FPS). Such systems frequently are held together only by gravity and friction (e.g. “dry masonry” construction structures [2]). A famous antique object, proved by time for durability, is chosen as example to provide FPS simulation. It is marble facade of the Parthenon Temple in the Athen (fig. 1), which had built from the precise blocks and drums freely standing on each other [3].



Fig. 1. The view of the Parthenon Temple in the Athen (2019)

The work aim is to disclose the stress state of such unusual object by FEA simulation. The contact task is in the focus – a large number of contact pairs should be modeled for FPS systems. It is necessary to reveal pressure patterns between drums, contact sliding, contact opening spots et al.

Understanding of stress state in the columns is very interesting for mechanical engineers [4, 5]. Such systems successfully withstood against many external impacts (earthquakes, shocks, etc.).

### GEOMETRIC MODEL OF THE SYSTEM

The simulation needs a 3D geometric model of the system. The model is built by drawings from the 1920<sup>th</sup>, drew up by good-known Parthenon researcher and keeper N.Balanos. In this work the west Parthenon facade is considered (fig. 2). The main part of the facade is the colonnade of 12 columns with the 4.3 m distance between axes of neighboring columns. The main facade is created by 8 forward columns, among which as most important two central and two corner ones (mark 1 in fig. 2a), and else two rear columns named as end ones (mark 2 in fig. 2a). Parthenon’s peristyle behind end columns is out of simulation.

\* Belarusian National Technical University, Minsk, Belarus

\*\* Maritime University of Szczecin, Szczecin, Poland

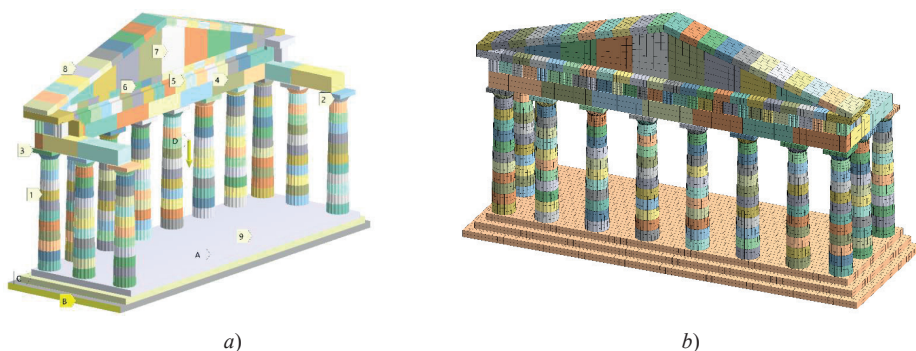


Fig. 2. Stylized full 3D-model of the Parthenon Temple facade (a) and its finite element model (b): A, B, C – marks of fastening, D – the mark of gravity force

Each column consists of 11 freely and precisely put on each other drums 1, and above them are echinus 2 and abacus 3. Those pillars are connected from above with each other by an architrave of marble blocks 4. The architrave is pressed down by blocks of frieze 5 and cornice 6. The system together of architrave, frieze, and cornice is called the entablature. Above the entablature on top of the facade there is triangle fronton 7, the slopes of which are covered by the roof blocks 8. At the bottom, the columns stand on the three-story stylobate 9 (three layers of stone slabs), and under the stylobate there is rigid rocky bed.

In the 3D-model the stylobate is created simplified as three huge plates (layers of 550 mm thickness), placed upon each other. All drums, echinus, abacus, entablature beams, fronton stones, and roof slabs are built as separate solids. All contact surfaces are plane everywhere. Each column has 10.425 m height and variable cross-section – diameter changes from  $\text{Ø}1.884$  m (bottom) to  $\text{Ø}1.46$  m (top). The mass of drums (numbered from bottom to top) changes from 5.12 to 3.31 tons. Sum mass of the column with echinus and abacus is equal 53.1 tons. Each of columns also has regular vertical grooves, the ridges between which are taking part in the compression stress concentration on the column ends. The full height of the 3D-model is equal 20.227 m. The sum mass of all blocks and drums (without the stylobate) reaches 1441 tons. Fronton and entablature jointly have mass of 756 tons.

Looking ahead it should be noted that the FEM results will show following: largest force (1153 kN) acts above the central columns, lesser force (692 kN) acts on the echinus of the corner columns, and just architrave marble block weight (mass of block – 24.5 tons) acts on the top of each of the end columns.

## TECHNICS AND CONDITIONS OF SIMULATION

Simulation is provided for the static conditions. It is possible to enhance the modeling scope onto transient processes (e.g. earthquakes). Hence, LBS of Pathenon has survived many shocks. So static analysis may be sufficient to point out the roots of system stability. The single external loading of Parthenon's facade are gravity forces. Preliminary FEM calculations show that after vertical gravity force applying there is no significant influence on the stress state from the side of the wind loading.

Facade is taken as carved from marble only, and some part of stylobate is presented by rocky bed material with decreased elasticity modulus (table 1). Marble is considered as a completely elastic material, obeying to Hook's law. Plastic deformations and fractures are not simulated. Geometrical nonlinearity is not included in the model. Single physical nonlinearity to simulate is the sliding friction according to Coulomb's law. The friction ratio is taken equal  $f=0.2$ . All contact surfaces are simulated as completely flat with ideal initial matching to each other. Roughness is not taken into

account. Rocky basement under stylobate is considered as absolute rigid (but able to incline – see below).

**Table 1.** Mechanical properties of the modeling materials

Property	Material	
	“Marble”	“Rock”
Elasticity modulus $E$ , GPa	30	10-20
Poisson’s ratio $\mu$	0.18	0.18
Density $\rho$ , kg/m <sup>3</sup>	2300	2500

It is accepted that compression stress becomes dangerous for strength of marble when it reaches 5 MPa [6, 7]. Thus, with a reasonable safety margin for brittle material, limit stress  $[\sigma_c]=2.5$  MPa is stated in this work [7, 8]. Minimum principal stress  $\sigma_3$  should not exceed that level (in absolute value) nowhere in the considered FPS system.

The simulation of full facade model (FM; fig. 2) is started from reduced model (RM; fig. 3). It gives possibility to understand stress state of the columns itself. The RM includes (fig. 3a) several separated submodels: triad of columns in the centre, pair of columns on the left, standalone corner column on the left. Triad and pair bear architrave blocks.

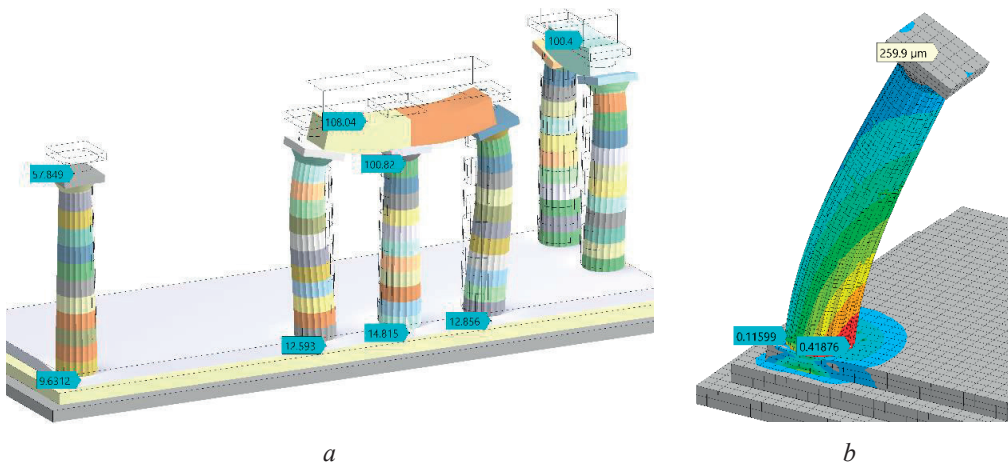


Fig. 3. Reduced model (RM) of Parthenon’s columns under gravity (a; marks mean total displacements in  $\mu\text{m}$ ) and equivalent stress  $\sigma_e$  (MPa) distribution (b) in the left standalone column under combination of gravity and wind pressure ( $p_w = 600\text{Pa}$ ):  $\times 18000$

Every solid possesses its own finite element mesh of volume type. Adjacent meshes are joined by contact pairs – two surface meshes, interacting with each other. All contact pairs in the model are switched to the status *frictional* to provide maximal reliability of the simulation.

Standalone column (fig. 3a) undergoes vertical compression mainly. It settles moderately (57.8  $\mu\text{m}$  only) when gravity is “switched on”. Architrave blocks additionally bend other columns. Vertical settlement of grouped columns became near doubled (100.8  $\mu\text{m}$ ).

Standalone column (fig. 3b) is loaded by wind from the left (additionally to the gravity). Hurricane-scale uniform wind pressure  $p_w = 600\text{Pa}$  causes some deflection of the column top (259.9  $\mu\text{m}$ ). However wind is not able to open contacts between drums. Wind-ward side of the column (left side) is still under gravity compression (0.115 MPa). Compressive stresses on the leeward side (right side) are evidently higher (0.418 MPa). Still stress state is far from dangerous squeezing. Therefore, wind loading is not the issue for represented columns.

Frictional contact pair is able to open, creating a gap (e.g. opened butt *a* in fig. 4), or to stay in a tightly closed state (mark 0.28 in fig. 4), where the *Surface Compression Concentrator* (SCC) is

visible along the junction outline of top drum and echinus. Let's name the outline SCC as SCC-1. One more example of the closed contacts – compressed drum's butts near the mark 0.22 in fig. 4.

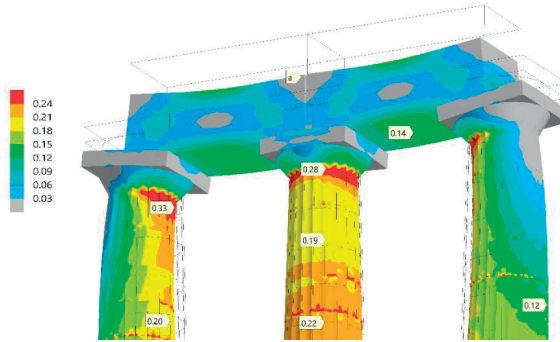


Fig. 4. The geometry of the columns' triad and equivalent stress  $\sigma_e$  (MPa) distribution under the gravity of two architraves and self-weight;  $\times 8500$

The model of marble facade is rigid fastened at the bottom to the three-layers stone stylobate by slipping fixation. There isn't significant difference between variants of applied fastening, but it should be normal to the surfaces of three stone slabs.

### COLUMN STRESSES AND CONTACT EFFECTS (REDUCED MODEL - RM)

The picture of principal stresses is given in fig. 5. One-axis compression dominates in the columns – vectors of minimum principal stress  $\sigma_3$  are vertically oriented (mark *d*). Architrave blocks undergo bending. Their top faces are compressed – vectors  $\sigma_3$  are only visible near mark *b*. The bottom architrave faces are, vice versa, tensioned. The mark *a* points to maximum principal stress  $\sigma_1$ .

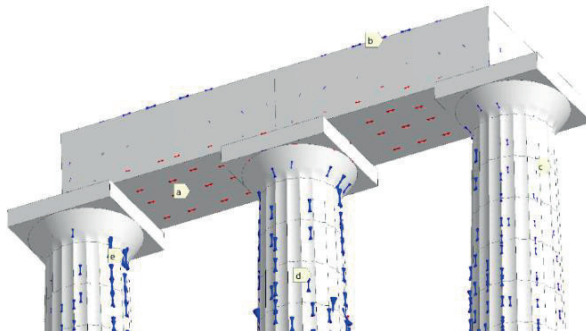


Fig. 5. Vectors of the principal stresses  $\sigma_1$ ,  $\sigma_2$ ,  $\sigma_3$  (red, green, blue colors respectively) for triad, standing under gravity force; RM,  $\times 1$

Compression is relatively weak (0.12 MPa; fig. 4) on the outer sides of the lateral columns. On the contrary, there is strong concentrator (0.33 MPa) of arcuate shape on the inner side of lateral columns, near “top drum–echinus” junction. Let's name the arcuate SCC as SCC-2. At the four drums distance down, the stresses lower in 1.65 times to 0.20 MPa.

For the middle column in the fig. 4, interesting sequence is observable while moving from top to bottom. The stresses peak (0.28 MPa) in the SCC-1 quickly weaken at the two drums distance down and became near evenly distributed in the section (0.19 MPa). Else two drums below, the stresses slight grow (0.22 MPa), what is caused by increasing of marble mass upon considered section.

Distribution of the minimum principal stress  $\sigma_3$  (fig. 6,a) is in accordance with the proposed conclusions. Compression stresses (mark *a*) in the rounded concentrator SCC-1 (between echinus and 11th drum) spreads at the top of the 8<sup>th</sup> drum (mark *b*). However, surface concentration appeared again on the 1<sup>st</sup> and 2<sup>nd</sup> drums (SCC-3). That effect is reflected in the contact spot (mark *c*) between column and stylobate.

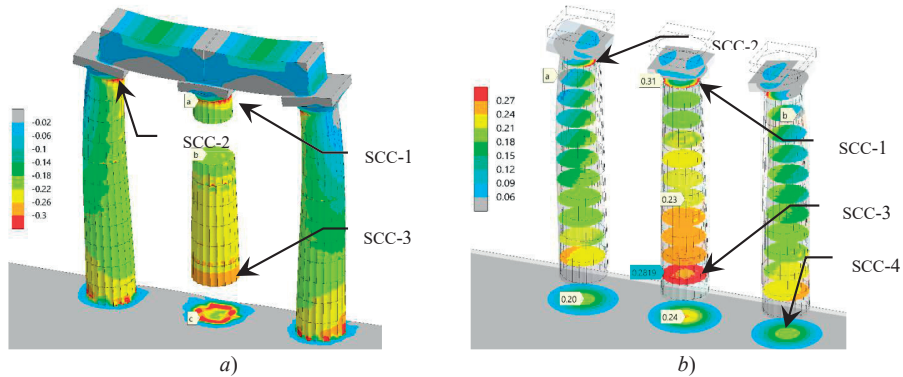


Fig. 6. Triad under gravity loading: *a* – picture of the minimum principal stress  $\sigma_3$  (MPa; drums 1, 2, 9, 10 not shown); *b* – contact pressure  $p_c$  on the junctions (two upper stores of the stylobate not shown); RM, MPa:  $\times 1$

Distribution of stress  $\sigma_3$  is near the same as contact pressure  $p_c$  picture presented on fig. 6b. For the middle column the scheme of events is following (chain of marks 0.31–0.23–0.28–0.24 MPa): rounded stress concentration below echinus (SCC-1) – stress levelling on the middle heights – rounded concentration above stylobate (SCC-3) – compression stress concentration in the center inside stylobate (SCC-4). The compression spreading in stylobate is quite moderate, and focusing of it is observed in the 2<sup>nd</sup> and 3<sup>rd</sup> stylobate layers – marks 0.20 MPa and 0.24 MPa relate just to the 3<sup>rd</sup> layer. The contact openings *a* and *b* are discovered in the top junctions of the lateral columns (10<sup>th</sup> and 11<sup>th</sup> drums). Those gaps are placed on opposite sides of columns and linked with SCC-2.

Thereby, compression localization in the FPS is linked to the edges of blocks/drums and spreaded on both surfaces, neighboring to the edge, but just on those surfaces to maximum. Simultaneously, some compression focusing may occur inside stylobate, deep under bottom drum. The rocky base is compressed unevenly, with spots of strong pressure below columns, but stylobate thickness is small enough to level pressure under it.

## THE FACADE STRESS STATE ANALYSIS (FULL MODEL - FM)

Figure 7 depicts Parthenon's facade as developed contact FEA-model. All stone parts – blocks and drums – are linked together only by contact pairs in frictional status. So full sticking is used for no one contact junction. It is important to note that the fronton center of mass is placed out of column axes plane, and removed forward on 20 mm according used drawing. That creates situation of the eccentric compression of columns.

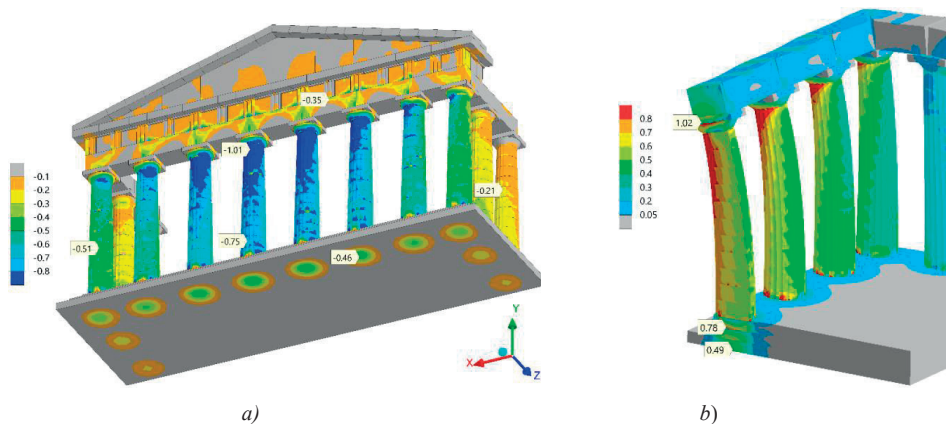


Fig. 7. Whole facade's minimum principal stress dispersion  $\sigma_3$  (a;  $\times 1$ ) and the picture of the equivalent stress  $\sigma_e$  (b;  $\times 3500$ ) for the sectioned colonnade. MPa; FM,  $\times 1$

One could see (fig. 7,b; the dispersion of  $\sigma_e$ ) central column bowing in the forward direction (to the left). It is observable owing to significant displacement scaling ( $\times 3500$ ). Fig. 7,a gives picture of  $\sigma_3$  on the natural scale ( $\times 1$ ), so bowing stayed imperceptible there.

Top forward sides of central columns are the most stressed region (-1.01 MPa in fig. 7,a) of the facade. Rounded concentrators SCC-1 are placed there. However, they are arcuate shape due to eccentric compression. As for 11<sup>th</sup> drum of a central column, minimum principal stress  $\sigma_3$  is 2.7 times lesser on the rear side than on the forward one.

On the central column has not shown a big difference in the compression stresses along any vertical flute. Mentioned stress  $\sigma_3=1.01$  MPa in fig. 7,a decreases only to 0.75 MPa (in 1.34 times) during descend to the bottom quarter of the column. Chain of mark 1.02–0.78–0.49 MPa for equivalent stress  $\sigma_e$  in same column section (fig. 7,b) points out strip of compression.

Thus, smooth lowering (in  $\sim 1.35$  times) of the average compression stress is observed during conditional descend from echinus to the stylobate. All columns act to the supposed rocky base in a concentrationly. Generated stresses penetrate through stylobate without significant changes (mark 0.46 MPa in fig. 7,a and mark 0.49 MPa in fig. 7,b).

Corner columns compressed half as weak (-0.51 MPa), than central ones, and the end columns are loaded mainly by their own weight – in them arise a little stressed (-0.21 MPa). A comparison of stress states for different columns points out the importance of the stone fronton gravity.

Pay attention to the triangle *a–b–c* in fig. 8, which embraces half of the fronton.

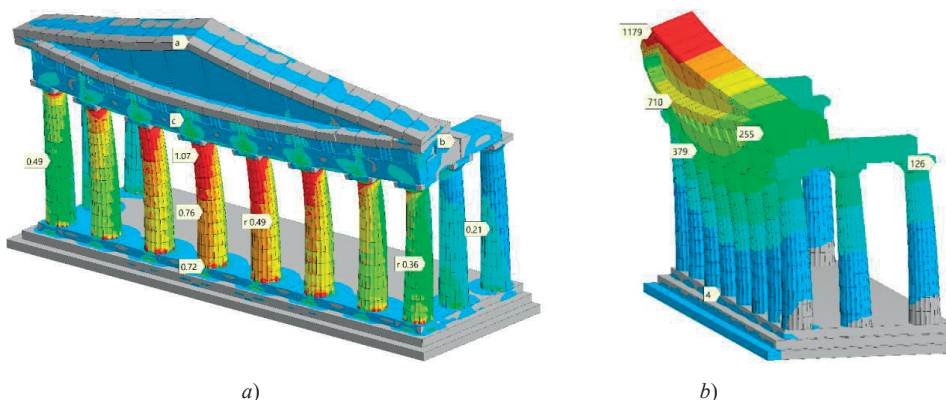


Fig. 8. Distribution of equivalent stress  $\sigma_e$  (a; MPa; color scale) and deformational displacement of the facade (b;  $\mu\text{m}$ ) under self-weight; FM,  $\times 3500$

By the point *b* marked the opened contact between architrave blocks. Point *a* is the vertex of the facade. It displaced forward on 1179  $\mu\text{m}$  (fig. 8b). Point *c* (on the frieze middle) moved only on 710  $\mu\text{m}$ . A comparison of marks 710  $\mu\text{m}$  and 255  $\mu\text{m}$  (at the frieze end) points out bulging of facade to forward (additionally to bowing). Central column tops moved forward at 379  $\mu\text{m}$ .

Pictures of stress  $\sigma_3$  (fig. 7a) and  $\sigma_e$  (fig. 8a) are very similar. Hence, equivalent stress is formed mainly by compression. Stresses from opposite sides of the central column (for 6<sup>th</sup> drum) marked by the paired marks 0.76 MPa and r 0.49 MPa. Stress difference discloses the influence of the eccentric compression.

Marks 0.49 MPa and r 0.36 MPa create a similar pair for the corner columns.

Facade's load-bearing system deformation may be depicted by contact slipping (fig. 9). Strictly vertical facade position is shown in fig. 9a. Figure 9b corresponds to the hypothetical inclination to forward at 3° (due to movement in rocky base e.g.). Dangerous slope (main discussion at the paper end) causes slippage growing in several times. It is likely, that during further slope (as uncontrolled sliding of blocks and drums) the facade destruction will begin.

There is a principal difference between fig. 9a and fig. 9b. Every column in fig. 9a possess its own picture of contact slipping. At the same time, all stones stay together, in the jointed system. After inclination, in fig. 9b, all facade columns deform uniformly. However, they evidently separate from end columns, where the peak of slippage (1157  $\mu\text{m}$ ) is observed, and the full opening of the corresponding contact pair took place.

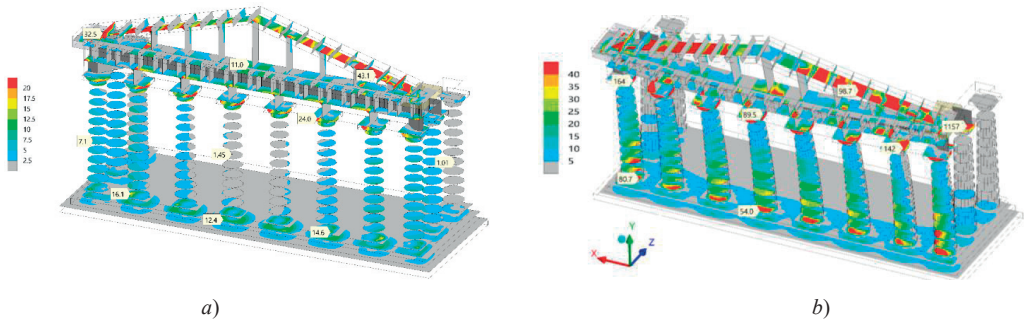


Fig. 9. Sliding ( $\mu\text{m}$ ) distribution in the facade's contact pairs: *a* – vertical position ( $\times 1$ ); *b* – the inclination to forward at 3° ( $\times 350$ ); FM

Slipping pictures became very similar for all eight facade columns (fig. 9b). Every column bottom (1-st drum) slips intensively to forward on stylobate (54.0  $\mu\text{m}$  e.g.). Incompatibility of fronton-colonnade deformations is growing. It is revealed by high values of slipping (164  $\mu\text{m}$ , 89.5  $\mu\text{m}$ , 142  $\mu\text{m}$ ) between abacus (belongs mostly to the colonnade) and all entablature (joined with the fronton).

Comparatively to fig. 9b high stability is visible in fig. 9a. The main feature of the situation – small, maybe negligible, slippage in the central column junctions (1.45  $\mu\text{m}$ ). It points out to the column stability despite the some loading eccentricity.

As for the central part of facade, significant contact slipping occurs:

- above column top, where abacuses and architraves are mutually adopting (24.0  $\mu\text{m}$ );
- between column's bottom drum and 3 stylobate stores (12.4  $\mu\text{m}$  и 14.6  $\mu\text{m}$ );
- on the border between fronton and entablature (11.0  $\mu\text{m}$ ).

Roof plates slipping (43.1  $\mu\text{m}$ ) is the main movement at the fronton corners. Simultaneously roof plates shift relative to each other (32.5  $\mu\text{m}$ ). Only corner columns significantly lean forward. It causes large slipping (7.1  $\mu\text{m}$ ) between their drums. Therefore, facade's parts adopt actively to the loading applied.

End columns stand almost unmovable. The slippage between drums is minimal (1.01  $\mu\text{m}$ ).

Figure 10 shows pressure distribution in the inner column junctions. Eccentric compression of the central column changes SCC shape from circular to arcuate one. Discussed above SCC-1 now is placed near mark 0.92 MPa. Mark 0.71 MPa points out to the transformed SCC-3.

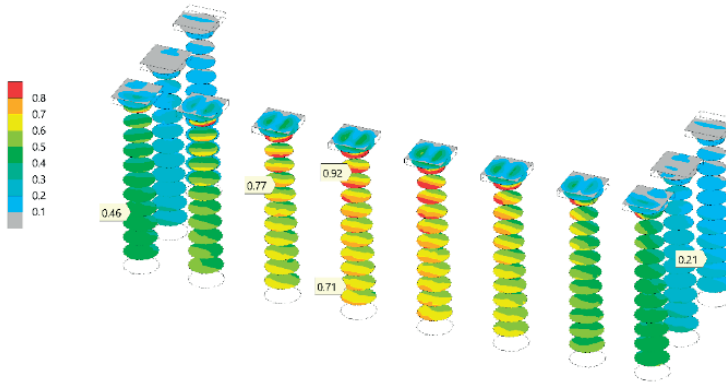


Fig. 10. Contact pressure  $p_c$  (MPa) between column drums; FM,  $\times 1$

Corner column butts (0.46 MPa) are compressed relatively evenly. It relates mainly to the bottom parts of the columns. End columns are carried away after the leaning façade. That is why local pressure  $p_c$  pictures acquired the arcuate shape again (0.21 MPa).

Opening junctions of drums are observed only in the end columns (fig. 10). The façade itself is monolithic and stable enough in spite of eccentric loading from above, due to the mentioned shift of the fronton point of mass. That conclusion is relevant only for precisely vertical column positions.

At the end of the work, the hypothetical situation of the façade inclination was investigated. It may occur as consequence of an earthquake or landslide, e.g. The gravity force vector was rotated step by step to the rear side. It is equivalent to façade's lean to forward. The critical situation is stated for the  $3^\circ$  inclination (fig. 11).

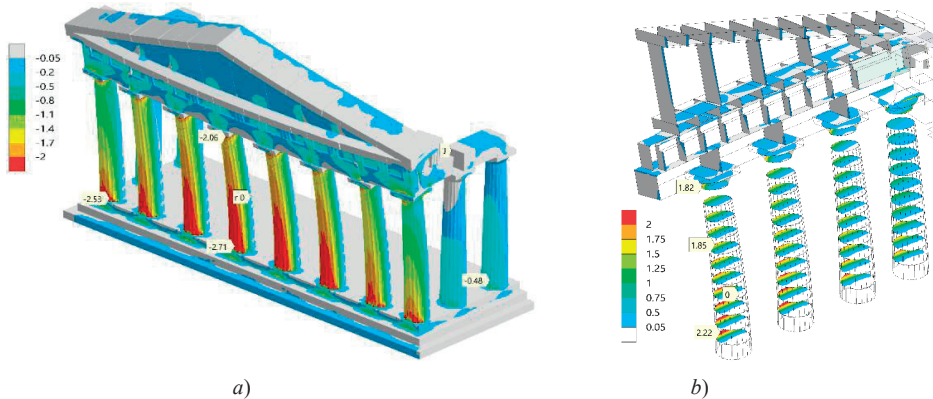


Fig. 11. Picture of the minimum principal stress  $\sigma_3$  (a) for façade in the case of  $3^\circ$  inclination to forward and the related distribution of contact pressure  $p_c$  (b) in the column sections. MPa; FM,  $\times 350$

Inclination is amplified by eccentricity of the loading from fronton weight and self-weight of columns. Inclination amplified eccentricity of the column loading by fronton and self-weight. It's caused high (in absolute value) level of minimum principal stress  $\sigma_3$  (fig. 11a): -2.71 MPa at the central column bottom and -2.53 MPa at the corner one. That stresses (of SCC-3 type) exceed the limit stress  $[\sigma_c]=2.5$  MPa. Thus, chipping of the stone becomes the real threat. SCC-1 exists due to inclination providing the echinus compression (-2.06 MPa).

Dangerous compression warning relates to the forward column sides. Rear sides are fully unloaded (mark **r0**). It happens due to the opening of all drum junctions, where contact pressure  $p_c$  picture (fig. 11b) indicates zero value at the about half area of each contact (mark **0**). Gaps reach here around several tens of micrometers. One of the sequences of large-scale junction openings is decrease of the facade rigidity (in all directions). On the forward column side, the contact pressure is localized in small segments (marks 1.82, 1.85, 2.22 MPa from top to bottom). High pressure is dangerous for a fragile drum/block material and may activate the contacts crush mechanism.

After all, Parthenon's facade is stable in the vertical position and durable, though too vulnerable to the hypothetical inclination even at small angle. Limit ( $3^\circ$ ) exceeding leads to the uncontrollable sliding at the column butts and whole structure disintegration.

## CONCLUSIONS

Load-bearing system of Parthenon's facade as FPS type was simulated by FEA. The eccentricity of fronton (20 mm forward) is taken into account. Stress state is depicted, including smooth lowering (in  $\sim 1.35$  times) of the average compression stress from echinus to the stylobate.

Sequences of the contact sliding and shifts are described. Different contact interaction patterns are revealed. The adaptive character of the contact slippage picture was considered. The presence of numerous contact gaps in the compressed system is stated as natural feature for FPS.

The surface compression concentrators (SCC) as a special class of stress concentrators are depicted. They are tied to blocks/drums edges, occupying both free and interacting surfaces. Rounded and arcuate SCC easily transforming into each other are potentially dangerous for compressed material at least for local overstraining. The significance of that class of concentrators is underestimated, because the SCC may be compatible (under some conditions) with longevity of constructure.

Column ends, near echinus and near stylobate, are the SCC places. The periodical transition from SCC to stress leveled regions and back again is revealed along column height. Moderate self-focusing of the compression stress is stated inside stylobate under columns.

Eccentric compression of the columns caused due to fronton eccentricity is simulated, and response of drums contact pairs is discovered. The simulation predicts Parthenon's facade vulnerability to the inclination from vertical. Beginning from  $3^\circ$  level, uncontrollable deformation by sliding and local crashing is expected. Slippage localization on the column bottoms, about abacus and in the fronton corners is the predictor of the upcoming instability.

## References

- [1] Zienkiewicz, O.C. and Taylor, R.L. (2000) *The finite element method*. Oxford: Butterworth-Heinemann, Vol. 1 Basis.
- [2] Brooks, A. and Adcock, S. (2013) *Dry stone walling, a practical handbook*. TCV.
- [3] Beard, M. (2003) *The Parthenon*. Cambridge: Harvard University Press, 209 p.
- [4] Downar, S., Jakimowicz, A., Jakubowski, Cz., Jakubowski, A. (2016) *Conception of simultaneous teaching the students of direction "Machine design" to three-dimensional modeling and virtual testing by FEM-analysis*. General and professional education, Vol. 1, pp. 26-32.
- [5] Downar, S., Jakimowicz, A., Jakubowski, A. (2017) *Methodology of mechanical student quick involvement into CAD- and CAE-area simultaneously*. General and professional education, Vol. 3, pp. 11-17.
- [6] Roca, P., Cervera, M., Gariup, G., & Pela', L. (2010). *Structural analysis of masonry historical constructions. Classical and advanced approaches*. Archives of Computational Methods in Engineering, 17(3), 299–325. <http://doi.org/10.1007/s11831-010-9046-1>
- [7] Natalia E. Lozano-Ramírez. (2015) *Finite element modeling of existing masonry towers: The Asinelli tower*. Thesis for: Dottore magistrale in Architettura costruzione città. Advisor: Stefano Invernizzi. POLITECNICO DI TORINO. Faculty of Architecture. Turin, Italy.
- [8] Stefano Invernizzi, Giuseppe Lacidogna, Natalia E. Lozano-Ramírez, Alberto Carpinteri. (2019) *Structural monitoring and assessment of an ancient masonry tower*. Engineering Fracture Mechanics, Vol. 210, pp. 429-443, ISSN 0013-7944. <https://doi.org/10.1016/j.engfracmech.2018.05.011>